Pergamon

Polyhedron Vol. 14, No. 13–14, pp. 1929–1935, 1995

0277–5387/95 $9.50+0.00

0277-5387(94)00446-3

ELECTROCHEMICAL, SPECTROELECTROCHEMICAL AND X-RAY ABSORPTION SPECTROSCOPIC STUDY OF SOME IRON(II) AND IRON(III) POLYPYRAZOLYLBORATO COMPLEXES

S. ZAMPONI, G. GAMBINI, P. CONTI, G. GIOIA LOBBIA and R. MARASSI*

Dipartimento di Scienze Chimiche, Università di Camerino, 62032 Camerino, Italy

M. BERRETTONI

Dipartimento di Matematica e Fisica, Università di Camerino, 62032 Camerino, Italy

and

P. CECCHI

Dipartimento di Agrobiologia ed Agrochimica, Università della Tuscia, 01100 Viterbo, Italy

(*Received* 6 *September* 1994; *accepted* 24 *October* 1994)

Abstract—The electrochemical, UV–vis spectroelectrochemical and X-ray absorption spectroscopic characterization of some polypyrazolylborato complexes of iron(II) and iron(III) are reported. The UV–vis spectroelectrochemical results have shown that changes in spin state occur during electrochemical oxidation of some iron(II) complexes. The results of the UV–vis experiments have been correlated with the features of the X-ray absorption spectra recorded on the powdered compounds in the XANES region.

Trispyrazolylborato ligands with a number of different (organo) metallic ionic counterparts[1] have been investigated extensively since their discovery by Trofimenko.[2] The flexible tridentate mononegative ligands are ideally suited to replace two monodentate anions in a metal(II) coordination sphere, giving rise to a neutral, quasi-octahedral complex of the type $M[RB(pz)_3]_2$.[3] Iron derivatives, among several other possible complexes, have received particular attention because of spin-state equilibria highly sensitive to the ligand substitution pattern. The ground states of $Fe[HB(pz)_3]_2$ and $Fe[HB(3,5\text{-}Me_2pz)_3]_2$ are low spin ($^1A_{1g}$) and high spin ($^5T_{2g}$), respectively. Both compounds present temperature- (and pressure-) dependent spin crossover phenomena. The equilibria and the kinetics of spin crossover have been studied using a variety of techniques.[4] The occurrence of spin crossover seems to depend on the substituents on the pz ring or boron atom. In the latter case, for instance, the replacement of a hydrogen atom with a pyrazolyl or phenyl group (i.e. more electronegative groups) leads to low spin compounds, e.g. $Fe[B(pz)_4]_2$. The correlation between spin state and type and number of substituents on the pyrazole ring, especially in position 3, is less clear since steric effects on the metal centre may play an important role.[5] Spin state and number of substituents affect the Fe—N bond length, which in high spin $Fe[HB(3,5\text{-}Me_2pz)_3]_2$ is 19.9 pm longer than in low spin $Fe[HB(pz)_3]_2$.[6] In addition to spin crossover phenomena and the correlation between bond length and nature and position of the substituents, these compounds may be of biological and catalytic interest. $Fe[HB(pz)_3]_2$,

* Author to whom correspondence should be addressed.

Table 1.

Complex	Formula[a]
1aFe^{II}	$Fe[HB(pz)_3]_2$
1bFe^{II}	$Fe[B(pz)_4]_2$
1cFe^{II}	$Fe[HB(3\text{-}Mepz)_3]_2$
1dFe^{II}	$Fe[HB(3,5\text{-}Me_2pz)_3]_2$
2aFe^{III}	$Fe[HB(pz)_3]_2^+ BF_4^-$
2bFe^{III}	$Fe[B(pz)_4]_2^+ BF_4^-$
2cFe^{III}	$Fe[HB(3\text{-}Mepz)_3]_2^+ BF_4^-$
2dFe^{III}	$Fe[HB(3,5\text{-}Me_2pz)_3]_2^+ BF_4^-$

[a] $[HB(pz)_3]^-$ = hydridotris(1*H*-pyrazol-1-yl)borate.

for instance, has been found as a product of the reduction of a model compound of the diiron centre in hemerythrin[7,8] and has also been used in catalysis.[9]

This paper deals with the electrochemical and spectroscopic characterization of the iron(II) and iron(III) polypyrazolylborate complexes reported in Table 1. UV–vis spectroelectrochemistry has been performed using Optically Transparent Thin Layer Electrodes (OTTLE). X-ray absorption spectroscopy (XAS) in the XANES region has also been used to study the solid compounds.

RESULTS AND DISCUSSION

Electrochemical measurements

Figure 1 shows a cyclic voltammogram for compound **1a** in MeCN, 0.1 M TEAP, that is representative of the electrochemical behaviour of all the other solutes. For this particular compound, the curve is similar to that obtained by Armstrong *et al.*[9] Controlled potential electrolysis in thin layer cells (see below) shows that for all compounds the number of electrons exchanged in the electrochemical process is one, and therefore the electrochemical reaction may be written as

$$FeL_2 \underset{+e^-}{\overset{-e^-}{\rightleftharpoons}} FeL_2^+$$

where L is any one of the studied ligands.

The trend of the peak separation, over the scan rate range 50 mV s^{-1}–2 V s^{-1}, corresponds to the one expected for a process at the limit of quasi-reversible charge transfer.[10,11] This hypothesis has been verified by fitting the experimental data with a generalized simulator for quasi-reversible processes. A Simplex routine, included in the simulator, permits the measurement of relevant electrochemical parameters such as formal potentials and heterogeneous charge transfer rates. The program fits the experimental data with the simulated theoretical response and gives as output the relevant electrochemical parameters. Table 2 includes the formal standard potentials and the heterogeneous charge transfer rates as obtained from the simulator. The transfer coefficients have not been included as they are close to 0.5 for all compounds. The formal potentials relative to the complexes **1a** and **1b** are in good agreement with those reported in the literature.

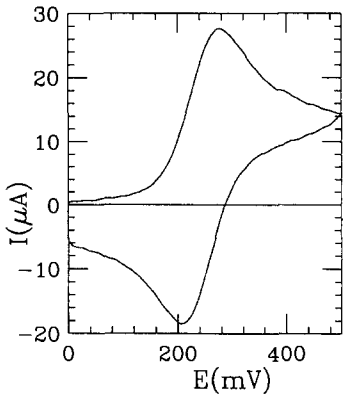

Fig. 1. Cyclic voltammogram obtained in a 1×10^{-3} M, 0.3 M TEAP, solution of **1a** at a platinum electrode. Scan rate 0.1 V s^{-1}.

Spectroelectrochemical measurements

More revealing from the point of view of the redox mechanism and of the fate of the compounds upon variation of the formal oxidation state of the metal are the spectroelectrochemical results. Two types of spectroelectrochemical measurements have been performed: slow scan rate potential sweep[12] and chronoabsorptometry.[13] The first technique, where the OTTLE potential is swept at low scan rate (1–2 mV s^{-1}), permits us to record simultaneously a thin layer voltammogram and a sequence of spectra at different potentials. In potential step chronoabsorptometry, the electrode poten-

Table 2.

Complex	$E^{\circ\prime}$ (mV)	$E^{\circ\prime}$ (mV)$_{\lambda_{max}}$	k° (cm s^{-1})
1a/2a	280 (230;[a]270[b])	275	0.013
1b/2b	380 (370[b])	385	0.013
1c/2c	410	403	0.013
1d/2d	220	215	0.015

[a] Ref. 2.
[b] Ref. 9.

tial is driven from the initial value, where no electrochemical reaction takes place, to selected values while recording spectra until a stable absorption profile is obtained. The absorbances at a convenient wavelength may be used to draw E vs log $(A_{Red}-A)/(A-A_{Ox})$ plots, where A_{Red} and A_{Ox} are the limiting absorbances of reduction and oxidation, and A is the absorbance at a certain intermediate potential. These are the optical analogues of the Nernst log plots,[13] from which n values and formal potentials may be computed. The number of electrons involved, computed from these plots, was equal to one for all complexes, in agreement with the controlled potential measurements. The formal potentials are listed in Table 2, together with those obtained from the cyclic voltammograms.

Figure 2 shows the spectra of solutions of complexes **1a**, **1b**, **1c** and **1d** in MeCN solution. As may be seen in the UV–vis region, all the spectra are characterized by an intense absorption band at 230 nm that has been assigned to the pyrazolic ligand absorption.[14]

Complexes **1a** and **1b**, which are in the low spin state,[15] present a shoulder at 286 and a band at 336 nm that may be assigned to absorption due to charge-transfer processes. In the spectra of the complexes **1c** and **1d**, these bands are absent because of the high spin state. The spectra obtained for compounds **1a**, **1b** and **1d** correspond to those of Jesson *et al.*,[14] in spite of the different solvents used.

Figure 3 shows the spectra of the ion(III) complexes in the same solvent. As may be seen, all the compounds are characterized by the presence of a prominent band at 230 nm and of an intense band in the visible region around 450 nm. The presence of this band indicates that, when the formal oxidation state of iron is three, all the compounds, under the stated experimental conditions, are in a low spin state. Compounds **1c** and **1d** change their spin states with changing iron oxidation state.

Spectroelectrochemical experiments demonstrate

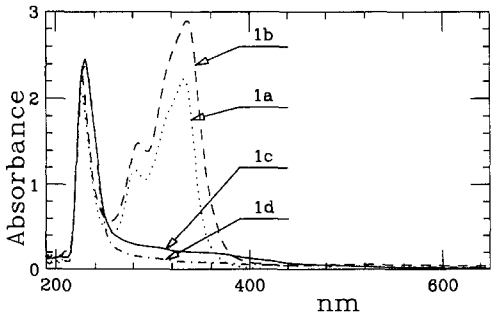

Fig. 2. Overlapped spectra of iron(II) complexes in acetonitrile solution normalized to the concentration.

Table 3. Band assignments

Complex	$\lambda_{max}(\varepsilon, dm^3mol^{-1}cm^{-1})$
1a	226 (7159); 282 (4035); 316 (6123); 334 (7666)
1b	228 (5605); 286 (3685); 316 (5637); 334 (7180)
1c	230 (11,810); 370 (886.5)
1d	230 (8484)
2a	234 (9646); 274 (4148); 442 (5610); 520 (1616)
2b	230 (9629); 276 (3459); 448 (4035); 528 (1313)
2c	230 (8289); 282 (2179); 454 (3356)
2d	230 (9601); 482 (404)

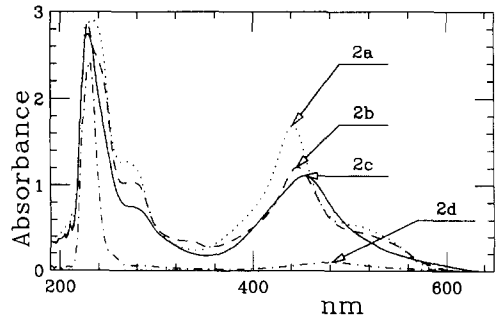

Fig. 3. Overlapped spectra of iron(III) complexes in acetonitrile solution normalized to the concentration.

that the same spin state variation occurs during electrochemical oxidation. Complexes **1a** and **1b** retain the same spin state configuration during oxidation (the same is true for compounds **2a** and **2b** during reduction). For compounds **1c** and **1d**, a spin state variation occurs during the oxidation. A similar consideration can be made for compounds **2c** and **2d** during reduction.

Figure 4 shows a sequence of spectra taken during a slow potential scan in an RVC-OTTLE for compound **1a**. The UV part of the spectrum, where no changes are observed during the potential scan, is not shown. The initial spectrum shows an intense band at 334 nm (typical of a low spin state), which decreases with increasing potential. The decrease of the band at 334 nm occurs simultaneously with the growth of a broad band at 450 nm, consistent with the retention of a low spin state in the oxidized state. The presence of the isosbestic point is consistent with the simultaneous presence of two species in equilibrium.[16,17] The spectra obtained during the reverse potential scan are the mirror image of those in Fig. 4. The trend of the spectra obtained during a slow potential scan for compound **1b** is similar to that of **1a**, as would be expected from the previous results in solution for the native compounds.

Figure 5 shows a sequence of spectra of com-

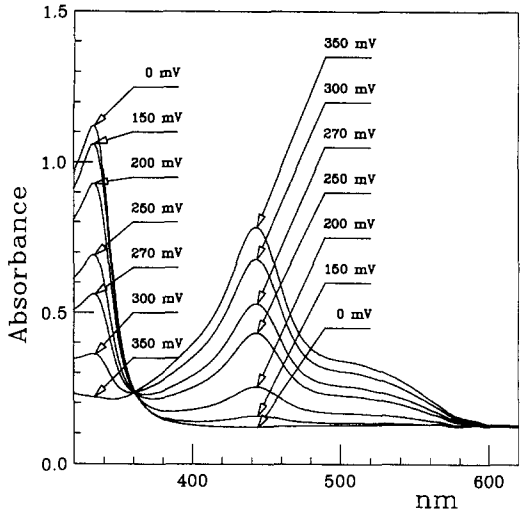

Fig. 4. Sequence of absorbance spectra taken during a 1 mV s^{-1} potential scan in a 1×10^{-3} M, 0.3 M TEAP solution of **1a** (see text for details).

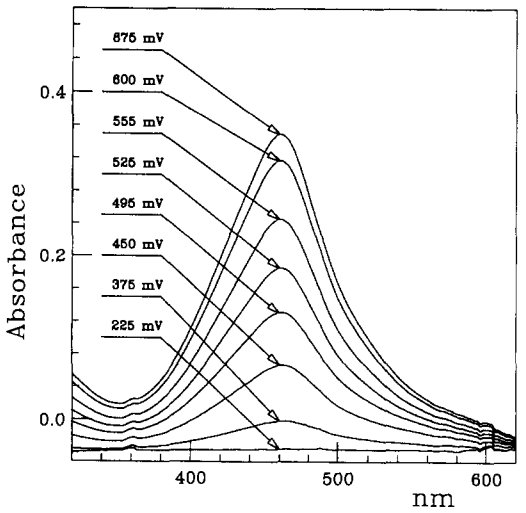

Fig. 5. Sequence of absorbance spectra taken during a 1 mV s^{-1} potential scan in a 4×10^{-4} M, 0.1 M TEAP solution of **1c** (see text for details).

pound **1c** obtained as described for compound **1a**. The initial spectrum is flat in the wavelength region shown. A broad band at 454 nm, similar to that observed for complex **1a**, grows progressively with increasing potential, demonstrating that the compound, initially in the high spin configuration, changes its spin state upon oxidation. Also, for complex **1c** the spectra taken during the reverse scan are the mirror image of those obtained during the forward scan. The trend of the spectra for compound **1d** is similar, the only difference being a red shift of the band ($\lambda_{max} = 482$ nm).

The spectra taken during the spectroelectrochemical experiments were elaborated to obtain corresponding thin layer voltabsorptometric curves.[12] A plot of $|dA\lambda/dt|$vs$E$ has the shape of a thin layer voltammogram and is generally "cleaner" because absorbances are insensitive to background contributions. The formal standard potential values measured from the voltabsorptometric curves are listed in Table 2. As may be seen, they are in fair agreement with the corresponding parameter obtained from the cyclic voltammograms.

XAS measurements

Figure 6a and b show the iron K-edge XANES spectra and the corresponding derivative curves of the powdered iron(II) complexes. Compounds **1a** and **1b** show a well-defined shoulder in the pre-edge region, clearly detectable in the corresponding derivative curves. The presence of this feature corresponds, in terms of UV–vis spectra, to the band around 340 nm found in both compounds and is characteristic of the low spin state. In the high spin

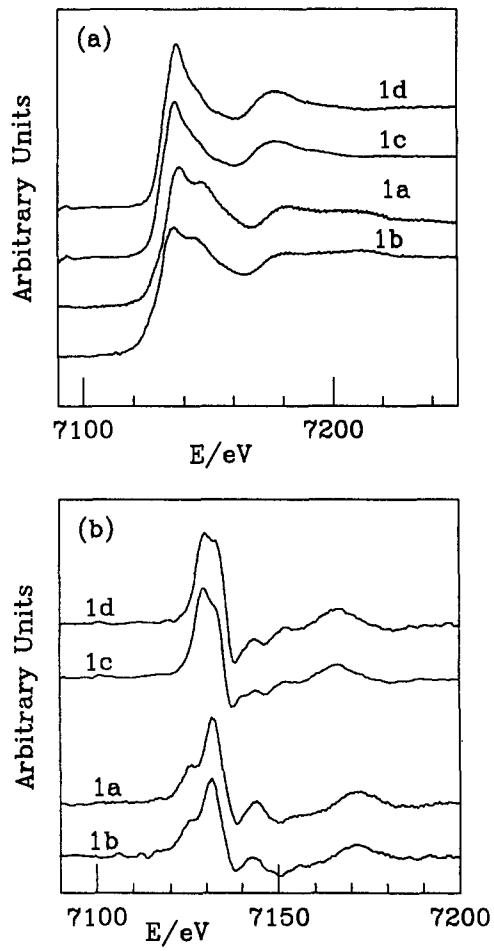

Fig. 6. XANES spectra and corresponding derivatives of the iron(II) complexes (see text for details).

compounds **1c** and **1d** the absence of any band in the visible region corresponds to a featureless pre-edge XANES spectrum. Figure 7 shows the XANES iron K-edge spectra (a) and the corresponding derivative (b) for the iron(III) complexes. As from the UV–vis results, these compounds are, under the stated experimental conditions, in a low spin state and, hence, the XAS spectra present a shoulder in the pre-edge region, as in compounds **1a** and **1b**. The shoulders in the pre-edge region may be assigned to the electronic transition ($1s \rightarrow 3d$) which, although theoretically possible in both spin states, is only observed in the low spin state compounds. The formally forbidden electronic transition probably occurs because of the partial $4p$ character of the $3d$ iron orbital due to the interaction with the π-orbitals of the pyrazole ligands.

With reference to the compounds **1a** and **1d**, the differences in the spectra may be explained taking into account the Fe—N bond lengths, which are known to be 19.7 and 21.7 pm, respectively, from X-ray measurements.[6] The elongation of the Fe—N bond is directly related to the spin state induced by the different electronic properties of the pyrazole rings due to the inductive effect of the methyl groups in positions 3 or 3,5. As a result of the increase of about 10% of the first coordination shell distance, the overlapping of the $3d$ iron orbitals with the π-orbital of the ligands decreases, preventing the occurrence of the $1s \rightarrow 3d$ electronic transition in the pre-edge region of the XAS spectra. The variation in the Fe—N bond length also causes a shift toward lower energy of the K-edge.[18] This is clearly shown by the spectra in Fig. 8, which have been taken in a differential mode, thus assuring the exact correspondence of the energy scale in the two spectra. Similar considerations may be applied to the other compounds for which the structure is not refined.

For the compounds with iron(III), the only refined structure is that of **2a**, for which the reported Fe—N bond length is 19.6 pm,[19] practically equal to the analogous iron(II) complex. This means that the presence of the forbidden $1s \rightarrow 3d$ transition may be explained as before. For the other iron(III) compounds, for which the structure is not refined, one may observe that the energy of the first oscillation of the XANES spectra is very sensitive to the first coordination shell distance, especially in the case of perfect octahedral symmetry.[18] As the energy of the first oscillation is the same in all compounds (see Fig. 7), one may safely assume that the average first coordination shell distance is very similar in all compounds, i.e. close to 19.6 pm. As

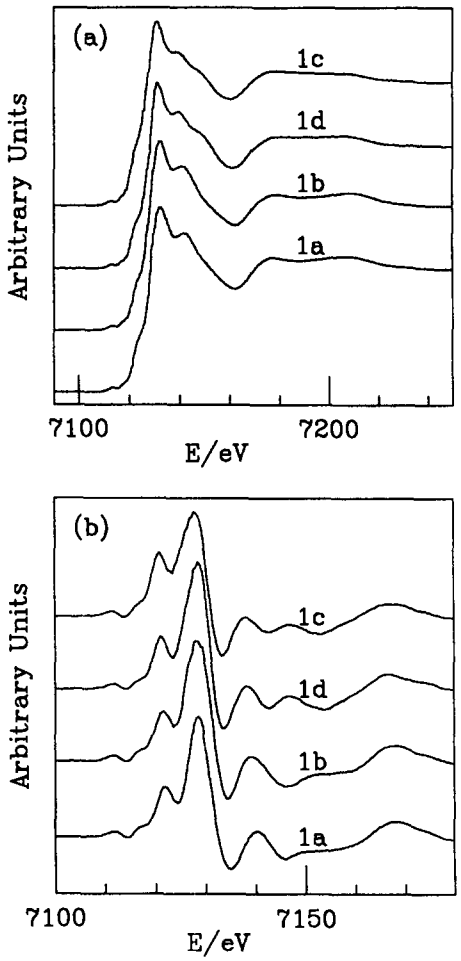

Fig. 7. XANES spectra (a) and derivative spectra (b) of the iron(III) complexes.

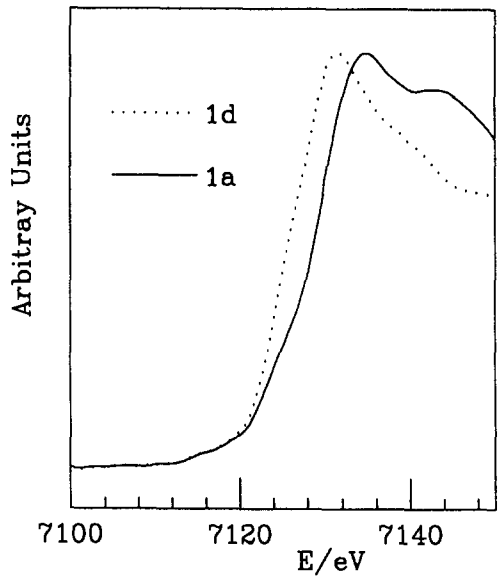

Fig. 8. XANES spectra in the edge region for compounds **1a** and **1d**.

a consequence one may conclude that, in iron(III) complexes, the pyrazole substituents are not very significant in promoting the increment of the Fe—N bond length.

This leads to the probable conclusion that the steric effect caused by the introduction of methyl groups on the pyrazole ring in iron(III) complexes, or in low spin iron(II) compounds, is probably not the main cause of variations of the Fe—N bond length, the spin state being the most important factor. This is also the case for nickel complexes analogous to **1a** and **1c**, where the metal does not undergo any spin change and the elongation of the Ni—N bond with changing substituent pattern in the pyrazole rings is negligible.[20]

Further XAS measurements of these and similar compounds, including complete analysis of the XANES and EXAFS regions, are in progress and will be the subject of a further communication.[21]

EXPERIMENTAL

Materials

All iron(II) polypyrazolylborate complexes were prepared according to Trofimenko.[2]

Synthesis of iron(III) *bis*[*hydridotris*(1H-*pyrazol*-1-*yl*)*borate*]*tetrafluoroborate* (**2a**)

In a flask containing 3.19 g of Fe_2O_3 (20 mmol) were added under stirring 3.14 cm^3 of 48% (by weight) HBF_4 (240 mmol) water solution. The mixture was left under stirring until all the solid was dissolved. The solution was then divided into four portions, each containing 10 mmol of $Fe(BF_4)_3$.

A solution of 5.04 g of potassium hydridotris(1*H*-pyrazol-1-yl)borate in 100 cm^3 of deionized water was added dropwise under stirring to one portion of the $Fe(BF_4)_3$ solution. A scarlet precipitate formed immediately. The precipitate was collected, washed with water, dried in a desiccator and recrystallized by slow evaporation from a dichloromethane–methanol (10:1, v/v) solution

Compounds **2b**, **2c** *and* **2d**

Iron(III) tetrakis[(1*H*-pyrazol-1-yl)borate]tetrafluoroborate (**2b**), iron(III) bis[hydridotris(3,5-dimethyl-1*H*-pyrazol-1-yl)borate]tetrafluoroborate (**2c**) and iron(III) bis[hydridotris(3-methyl-1*H*-pyrazol-1-yl)borate]tetrafluoroborate (**2d**) were prepared as for compound **2a** using the corresponding polypyrazolylborate potassium salts. Compound **2b** (red–brown). Found (Calc.): C, 44.0 (44.1); H, 5.0 (4.9); N, 25.6 (25.7). IR 2134 w, 2538 m (BH), 1502 vs, 1049 vs br (BF_4), 798 vs, 735 s. Compound **2c** (pale red). Found (Calc.): C, 48.6 (48.9); H, 6.1 (6.0); N, 22.6 (22.8). IR 3135 w, 2564 m (BH), 1540 s, 1066 vs br (BF_4), 819 s, 792 s. Compound **2d** (dark red). Found (Calc.): C, 41.0 (41.1); H, 3.5 (3.4); N, 31.7 (32.0). IR 3120 w, 1499 s, 1052 vs br (BF_4), 856 s, 792 m sh, 759 s.

Electrochemical and spectroscopic measurements

Glassy carbon (0.07 cm^2 area) and platinum (0.07 cm^2 area) disc electrodes were used for conventional cyclic voltammetric experiments. The OTTLE for spectroelectrochemical measurements was a 1×1.5 cm rectangular slice of reticulated vitreous carbon (RVC, $2 \times 1 \times 100$ ppi) 0.1 cm thick inserted at one end of a 5-cm-long quartz cuvette open at both ends.[12] Alternatively, the electrode was an 80:20 Pt–Rh alloy mesh (80 ppi) sandwiched between two microscope slides. The electrode assembly was held together with a Teflon frame without the use of any epoxy glue. The path length obtained using Teflon spacers was of the order of 0.2–0.25 mm. Both electrodes were used in a Teflon cell equipped with optical quartz windows. Details on the electrode construction and on the electrochemical cell may be found in Ref. 22.

A saturated calomel electrode (SCE) was used as reference in DMF (Fluka) solutions. When acetonitrile (water-free Aldrich HPLC grade) was used as solvent, the reference was an Ag/AgCl electrode in MeCN, separated from the main solution by a Vycor frit. Tetraethylammonium perchlorate (TEAP; C. Erba; 0.1 M for cyclic voltammetry and 0.3 M for spectroelectrochemistry) was used as supporting electrolyte.

An Amel System 5000 (Amel, Milan) was used for all the electrochemical measurements. The electrochemical curves were recorded directly on an *X–Y* recorder or stored on the system for further elaboration. The number of electrons (n) associated with each electrochemical process was measured using thin layer coulometry.

The electrochemical parameters, such as peak potentials, heterogeneous charge transfer constant etc., have been extracted from the experimental cyclic voltammograms using a generalized simulator coupled to a Simplex routine.

UV–vis spectra during spectroelectrochemical measurements were collected using an HP 8451A diode array spectrometer driven by an Amstrad 286 personal computer.

XAS measurements were taken at room temperature on the powdered compounds using an EXAFS laboratory machine (Rigaku) located at

the CIGA at the University of Camerino. Some spectra were also recorded at Adone storage ring in Frascati (Rome), at the Puls facility beam line equipped with a silicon (311) monochromator crystal that ensures rejection of high harmonics when the ring is operated at 1.1 GeV.

REFERENCES

1. (a) S. Trofimenko, *Chem. Rev.* 1993, **93**, 943; (b) S. Trofimenko, *Prog. Inorg. Chem.* 1986, **34**, 115; (c) S. Trofimenko, *Top. Curr. Chem.* 1986, **131**, 1; (d) S. Trofimenko, *Chem. Rev.* 1972, **72**, 497.
2. S. Trofimenko, *J. Am. Chem. Soc.* 1967, **89**, 3170
3. J. P. Jesson, S. Trofimenko and D. R. Eaton, *J. Am. Chem. Soc.* 1967, **89**, 3148.
4. (a) J. K. Beattie, N. Sutin, D. H. Turner and G. W. Flynn, *J. Am. Chem. Soc.* 1973, **95**, 2052; (b) J. K. Beattie, R. A. Binstead and R. J. West, *J. Am. Chem. Soc.* 1978, **100**, 3044; (c) E. V. Dose, M. A. Hoselton, N. Sutin, M. F. Tweedle and L. J. Wilson, *J. Am. Chem. Soc.* 1978, **100**, 1141; (d) B. B. Hutchinson, L. Daniels, E. Henderson, P. Neill, G. J. Lond and L. W. Becker, *J. Chem. Soc., Chem. Commun.* 1979, 1003; (e) F. Grandjean, G. J. Lond, B. B. Hutchinson, L. Ohlhausen, P. Neill and J. D. Holcomb, *Inorg. Chem.* 1989, **28**, 4406.
5. (a) T. Desmond, F. J. Lalor, G. Ferguson and M. Parvez, *J. Organomet. Chem.* 1984, **277**, 91; (b) see also W. H. McCurdy Jr., *Inorg. Chem.* 1975, **14**, 2292; (c) G. Gioia Lobbia, S. Calogero, B. Bovio and P. Cecchi, *J. Organomet. Chem.* 1992, **440**, 27.
6. J. D. Oliver, D. F. Mullica, B. B. Hutchinson and W. O. Milligan, *Inorg. Chem.* 1980, **19**, 165.
7. W. H. Armstrong and S. J. Lippard, *J. Am. Chem. Soc.* 1984, **106**, 4632.
8. M. Tachibana, K. Sasaki, A. Ueda, M. Sakai, Y. Sakakibara, A. Ohno and T. Okamoto, *Chem. Lett.* 1991, 993.
9. W. H. Armstrong, A. Spool, G. C. Papaefthymiou, R. B. Frankel and S. J. Lippard, *J. Am. Chem. Soc.* 1984, **106**, 3653.
10. H. Matsuda and Y. Ayabe, *Z. Elektrochem.* 1957, **59**, 494.
11. M. L. Olmstaed, R. G. Hamilton and R. S. Nicholson, *Anal. Chem.* 1969, **41**, 260.
12. S. Zamponi, M. DiMarino, R. Marassi and A. Czerwinski, *J. Electroanal. Chem.* 1988, **248**, 341.
13. W. R. Heinemann, F. M. Hawkridge and H. N. Blount, in *Electroanalytical Chemistry* (Edited by A. J. Bard), Vol. 13, pp. 1–113. Marcel Dekker, New York (1984).
14. J. P. Jesson, S. Trofimenko and D. R. Eaton, *J. Am. Chem. Soc.* 1967, **89**, 3158.
15. G. J. Long and B. B. Hutchinson, *Inorg. Chem.* 1987, **26**, 608.
16. D. M. Cohen and E. Fisher, *J. Chem. Soc.* 1962, 3044.
17. J. Brynestad and J. P. Smith, *J. Phys. Chem.* 1968, **72**, 296.
18. A. Bianconi, in *X-ray Absorption* (Edited by D. C. Koningsberger and R. Prins), Ch. 11, pp. 573–663. Wiley, New York (1988).
19. S. Calogero, G. Gioia Lobbia, P. Cecchi, G. Valle and J. Friedl, *Polyhedron* 1994, **13**, 87.
20. P. Cecchi, G. Gioia Lobbia, F. Marchetti, G. Valle and S. Calogero, *Polyhedron* 1994, **13**, 2173.
21. M. Berrettoni, S. Zamponi, R. Marassi, P. Checchi and G. Gioia Lobbia, unpublished work.
22. M. DiMarino, R. Marassi, R. Santucci, M. Brunori and F. Ascoli, *Bioelectrochem. Bioenerg.* 1987, **17**, 27.